(Invited Paper)

ULTRAFAST OPTICS IMAGING BASED ON POLARIZATION-DISCRIMINATION TECHNIQUES IN FILAMENTOUS TISSUES

CHIA-WEI SUN[1], C. C. YANG[1], YEAN-WOEI KIANG[1], CHII-WANN LIN[2]

[1]Graduate Institute of Electro-Optical Engineering, Graduate Institute of Communication Engineering and Department of Electrical Engineering, National Taiwan University,
[2]Institute of Biomedical Engineering, National Taiwan University, Taipei, Taiwan.

ABSTRACT

In this paper, we first demonstrated the effectiveness of imaging in a tissue phantom with isotropic scattering by using polarization discrimination combined with the time gating method. In this situation with lean pork as targets and diluted milk as tissue phantom, the reduced scattering coefficient mapping manifests clear images. However, such an imaging technique became less effective in filamentous tissues, such as chicken breast tissues, because filamentous tissue had a deterministically anisotropic property. It led to coherent coupling between the two linear polarization components. In this situation, we employed the time-gated degree of polarization (DOP) imaging technique that based on the Stokes formalism. The results showed that the DOP measurement was quite effective in high-quality imaging of objects in filamentous tissues. The improvement of this method was attributed to the unchanged polarization part under the coupling processes of various polarization components. Because the Stokes vector provides complete polarization information of transmitted light, this technique is quite effective for imaging and characterization in filamentous tissues.

Biomed Eng Appl Basis Comm, 2002 (December); 14: 237-242.
Keywords: time gating, polarization discrimination, optical imaging, filamentous tissue, degree of polarization

1. INTRODUCTION

Recently, biomedical imaging based on optical techniques has become an active area of research for developing medical diagnosis techniques. For thick biological tissues of several cm, ultrafast-optics techniques have been considered for optical imaging based on time-gated transmitted signals. In such a technique, psec or fsec pulses are applied to tissues and the transmitted quasi-coherent photons (snake photons) are extracted with various time-gating methods, including Kerr gating [1], stimulated Raman scattering gating [2], sum-frequency generation gating [3], optical parametric amplification gating [4], and the use of a streak camera [5]. Because there is no clear boundary between weakly scattered snake photons and strongly scattered or multiply scattered diffuse photons in the transmitted time-resolved signals, careful design and implementation of the aforementioned time gating techniques are required.

While time-gating methods have been proved useful for biomedical imaging, other optical gating techniques were developed to improve the resolution and contrast of images [6-11]. Among them, the polarization discrimination method is an important one [7-11]. This method is based on the depolarization effect in random scattering of tissues. In this effect, the input polarization state is partially preserved in weakly

Received: June 24, 2002; Accepted: Sept. 15, 2002
Correspondance: C.C. Yang, Professor
Dept. of Electrical Engineering, National Taiwan University, 1, Roosevelt Road, Sec. 4, Taipei, Taiwan,
E-mail: ccy@cc.ee.ntu.edu.tw

scattered photons. Thus, the quasi-coherent part can be extracted by transmitted co-polarized photons.

However, the measurement of the depolarization effect by discriminating coherent from incoherent photons becomes less effective when there exists coherent coupling between two perpendicular polarization components. Such coherent coupling phenomena can particularly occur in filamentous tissues with anisotropic structures. In this situation, the conventional polarization gating method becomes ineffective in optical imaging. In our study, we have found that by using the Stokes formalism, images of higher contrast and resolution in filamentous tissues could be achieved. In other words, images of the degree of polarization (DOP), based on the measurement of the Stokes vectors, manifest quite high quality in filamentous tissues.

In this paper, we report the developments of the aforementioned imaging techniques based on polarization manipulations of the transmitted signal through tissue samples in our laboratory. We will first show the advantages of time-gating and polarization discrimination in imaging objects in an isotropic turbid medium. Diluted milk was used as the medium for isotropic scattering. Then, we used chicken breast tissues, consisting of filaments with optically isotropic I bands (thin filament – containing actin) and anisotropic A bands (thick filament – containing myosin) [e.g., 12], as samples for demonstrating the failure of imaging in filamentous tissues when the aforementioned technique of combining time gating and polarization discrimination is used. Finally, the DOP was calibrated based on the measurements of the Stokes vectors for effective imaging in a filamentous tissue structure.

The results of isotropic tissue phantom image and optical characterization are shown in Sec. 2. Then, the imaging results of the conventional polarization gating approach based on snake photons in filamentous tissues are given in Sec. 3. Next, the time-resolved Stokes vector and DOP imaging method were shown in Sec. 4. Finally, conclusions are drawn in Sec. 5.

2. TIME-GATED IMAGE CHARACTERISTICS IN A PHANTOM OF ISOTROPIC SCATTERING

Figure 1(a) demonstrates the idea of an ultrafast optical imaging method with an input short pulse. The snake photons, i.e., the leading edge of the transmitted temporal profile, which pass through a turbid medium with fewer scattering events, carry more information of image. However, by including diffuse photons in imaging, strong random scattering blurs the image. The images shown in Fig. 1 were obtained by scanning a sample of diluted milk with 10 cm in transmission length. The pieces of lean pork were suspended in the diluted milk as scanning objects. The experimental details will be described later. In Fig. 1(b), with linearly polarized input signals, the transmitted co-polarized photons are more coherent and carry more information of tissue structures. The subtraction of the cross-polarized component from the co-polarized component, i.e., removal of the incoherent part, has been shown to be a useful procedure for effective optical imaging. In this imaging process, the depolarization factor was usually calibrated from measured data for image construction.

In the experimental setup for optical imaging with polarization-gated snake photons, as shown in Fig. 2, an Argon laser pumped mode-locked Ti:sapphire laser was used to provide 76 MHz, around 100 fsec laser pulses at 800 nm. The laser beam was split into three branches, one for triggering the used streak camera, the second for propagating through samples, and the third for temporal reference. About 200 mW average power was applied to the samples. Two polarizers, one before and the other after the samples, were used to control the input and output polarization for polarization discrimination. After the recombination of the sample and reference beams, signals were directed to

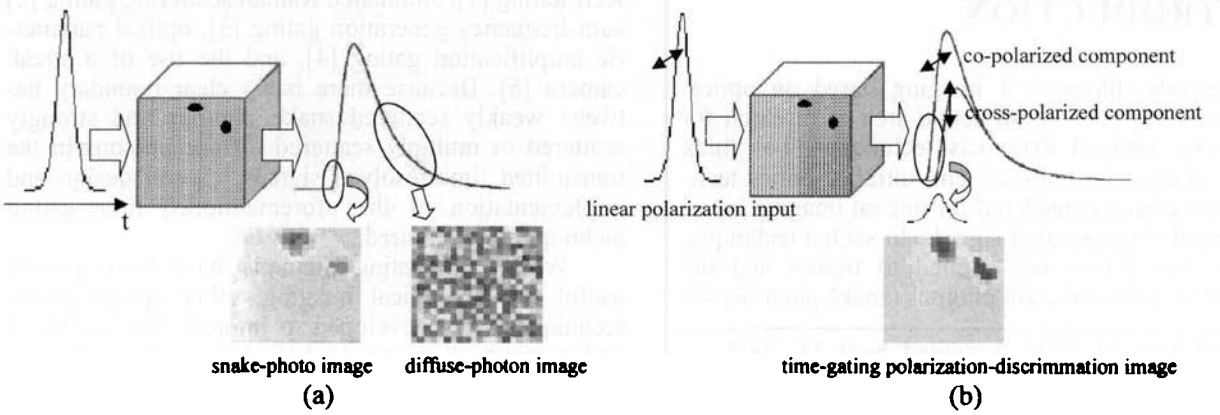

Fig. 1 Illustrations of (a) time-gating and (b) polarization-discrimination, time-gating techniques.

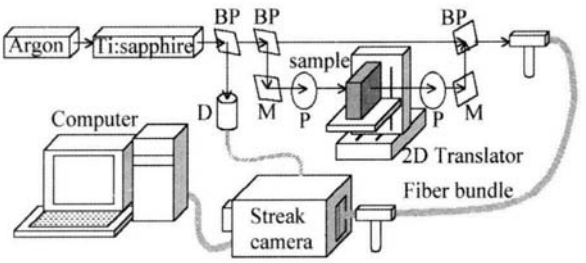

Fig. 2 Experimental setup. BP: beam splitter; P: polarizer; M: mirror; D: detector.

the streak camera with a fiber bundle. The temporal resolution of the operation mode of the streak camera was about 20 psec. This resolution limitation may partly be due to the group-velocity dispersion effect in the fiber bundle. The scanning mode was used in measurements, i.e., the fiber bundle end was always aligned with the incident laser beam while the samples were moved with a two-dimensional translation stage for image scanning.

In Fig. 3, two pieces of lean pork (2 and 1 mm in thickness, respectively) as objects were placed within diluted milk for imaging. The diluted milk was contained in a plastic vessel with the transmission length of 10 cm as tissue phantom. The scanning pixel size was 1 mm x 1 mm and the scanning area was 2 cm x 2 cm. Figure 3(a) shows the image of integrated intensity with appropriate time gating of I_p. Figure 3(b) shows the image of time-gated $I_p - I_c$, where I_p and I_c are co- and cross-polarized components of incident light, respectively. Although I_p can show the locations (red spots) of the two pieces of pork, $I_p - I_c$ does provide a clearer image, particularly for the smaller and thinner piece on the right.

To further understand the characteristics of the imaging mechanism with light transmission through a biological tissue with random scattering, the diffusion equation of total transmitted photons is adopted as follows:

$$\frac{1}{v}\frac{\partial \phi}{\partial t} - \nabla \bullet \left(\frac{1}{3(\mu_a + \mu_s')}\nabla \phi\right) + \mu_a \phi = I_s . \quad (1)$$

In Eq. (1), v is the speed of light in the medium, ϕ is the fluence rate of diffuse photon, and I_s is the source term of illumination photon. The absorption coefficient and reduced scattering coefficient are represented by μ_a and μ_s', respectively. We divided the fluence rate into two parts: an incident field that was excited by the original illumination source and a scattering field that was produced by the inhomogeneities. In an image reconstruction procedure [13], we solved Eq. (1) for absorption coefficient and reduced scattering coefficient with the time-resolved experimental data. Figure 4 shows the mapping images of absorption coefficient and reduced scattering coefficient based on

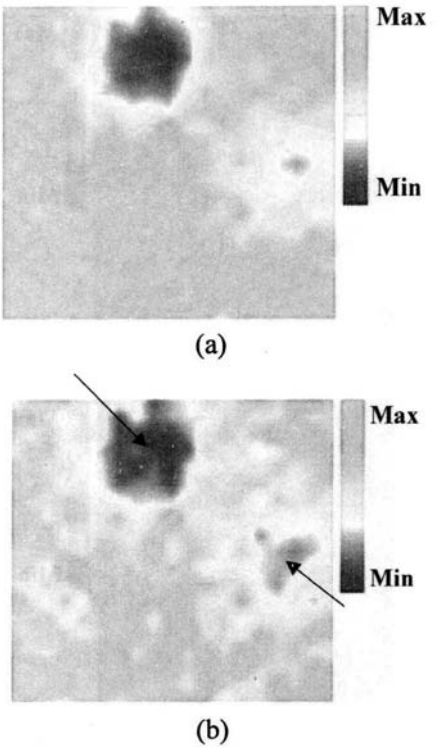

Fig. 3 Time-gated images of two pieces of lean pork in diluted milk with (a) I_p and (b) $I_p - I_c$.

the reconstruction procedure. One can see that the distribution of absorption coefficient does not reveal any significant information of the targets. On the contrary, the reduced scattering coefficient mapping provides a clear image. Therefore, the contrast of optical imaging with transmission measurement was furnished almost by the difference of scattering coefficient between targets (pork) and turbid background (diluted milk).

Because diluted milk represents a turbid medium of statistically isotropic scattering, the depolarization effect of transmitted signals is a good indicator of scattering strength. Therefore, the results of polarization discrimination manifest good images in this case. Particularly, the mapping of reduced scattering coefficient clearly indicates the locations and shapes of the targets.

3. POLARIZATION-DEPENDENT CHARACTERISTICS IN FILAMENTOUS TISSUE

The image results in the last section indicate that the combination of polarization-discrimination with the time-gating method improves image contrast in an isotropic tissue phantom. For the study in filamentous tissues, we used chicken breast tissues as samples in our experiments. The chicken breast tissue sample has

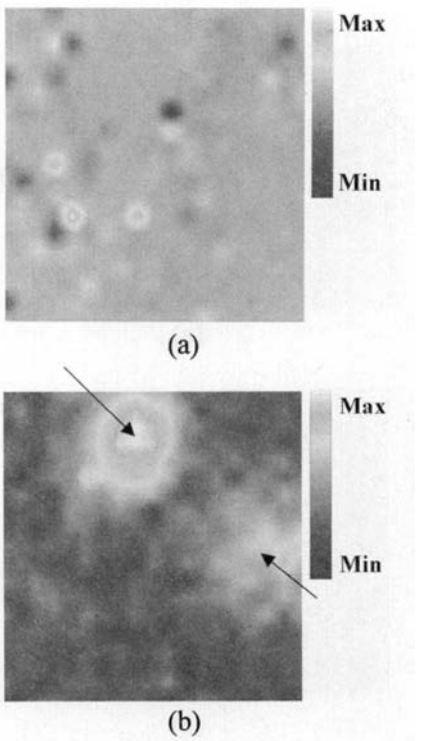

Fig. 4 Optical coefficients images of two pieces of lean pork in diluted milk with (a) μ_a and (b) μ_s'.

the thickness varying from 1.3 to 1.5 cm within the transverse scanning area. The imaging results with a thin chicken bone of diameter 1-2 mm (as the object) sticking into the breast tissue sample with the input linear polarization along the tissue filament direction are shown in Fig. 5(a) and (b). Parts (a) and (b) show the images of I_p and $I_p - I_c$, respectively. The result of I_p provides a rough picture of the chicken bone; however, $I_p - I_c$ leads to no feature at all. The imaging results confirm the coherent polarization evolution besides random scattering in skeletal muscle tissues. This indicates that besides possible random scattering in such a medium, coherent coupling between the two polarization components occurs due to the organized structure of the filamentous tissue. Due to certain coherent cross-polarized interactions, signal polarization seemed to rotate such that I_c became higher than I_p at the output. In this situation, both I_p and I_c were quite coherent, particularly before and near their peaks. Hence, the conventional polarization gating technique, i.e., imaging with $I_p - I_c$, became difficult.

4. TIME-RESOLVED STOKES VECTOR AND DOP IMAGE IN FILAMENTOUS TISSUES

As discussed in Sec. 3, deterministic optical birefringence results in coherent polarization evolution, leading to coherent polarization coupling and hence invalid coherent photon extraction through polarization discrimination. In this situation, all the elements of polarization state must be considered for understanding the polarization evolution and hence improving image quality in such a medium. In this section, we intent to apply the Stokes formalism for improving image contrast in the filamentous tissue.

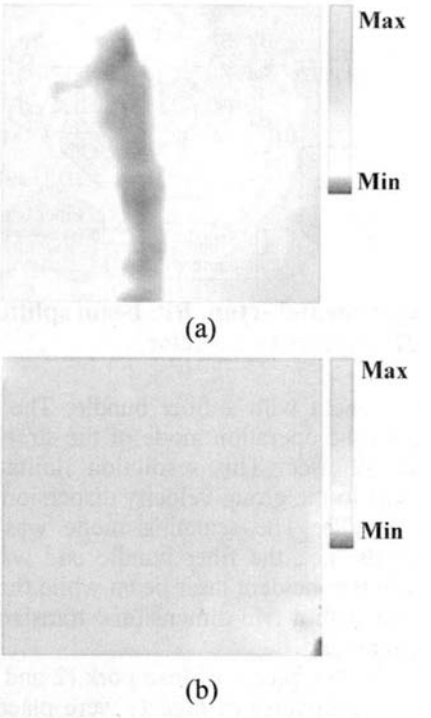

Fig. 5 Time-gated images of a chicken bone in chicken breast tissue with (a) I_p and (b) $I_p - I_c$.

The experimental setup is similar to Fig. 2, except that a quarter-wave plate was employed after samples for circularly polarized component measurements. According to the Stokes formalism, we need to measure four different polarization states of transmitted photons, including horizontal linear polarization component H, vertical linear polarization component V, 45° linear polarization component P, and right-hand circular polarization component R. In the experiments, such polarization control was accomplished through adjusting a polarizer and a quarter-wave plate. Here, the horizontal and vertical polarization directions are referred to the coordinate of the laboratory. The quasi-coherent photon data were obtained by gating the time-resolved intensity profiles with duration of 50 psec from the leading edges of the temporal curves.

The Stokes components, generally denoted by S_0, S_1, S_2 and S_3, form a sufficient set for describing the amplitude, phase and polarization of a light wave. To express the Stokes vector S in term of our experimental data, the following relation is established:

$$\mathbf{S}=\begin{bmatrix}S_0\\S_1\\S_2\\S_3\end{bmatrix}=\begin{bmatrix}H+V\\H-V\\2P-H-V\\2R-H-V\end{bmatrix}. \quad (2)$$

Here, S_0, S_1, S_2 and S_3 are proportional to the total intensity, the difference between the horizontal and vertical polarization components, the difference between the linearly polarized components oriented at 45° and -45°, and the subtraction of the left-handed from the right-handed circularly polarized components, respectively. Subsequently, we can calculate the DOP as follow:

$$\mathrm{DOP}=\frac{\sqrt{S_1^{\,2}+S_2^{\,2}+S_3^{\,2}}}{S_0}. \quad (3)$$

Again, we used chicken breast tissues of 1.5 cm in thickness as filamentous tissue samples in the experiments.

Figure 6 shows the time-resolved Stokes parameters of chicken breast tissue with the filaments along the horizontal polarization direction. The results were obtained with horizontally polarized incident pulses. The S_0 profile represents the total intensity of transmitted signal that contains quasi-coherent and diffuse photons. The S_1 profile is featureless because the mixed effects of coherent polarization coupling and random de-polarization process just result in almost cancellation between the H and V components in this case. Such featureless S_1 was the major reason for ineffective imaging operation based on polarization discrimination. On the contrary, the S_2 and S_3 profiles furnish the information of coupled polarization components of quasi-coherent photons. The depression features of S_2 and S_3 near the leading edges of the time-resolved profiles should result in more image information if the time-gated Stokes vector is calibrated.

To demonstrate the improvement of image contrast based on the time-gated Stokes vector, we stuck a thin chicken bone (its shape and size are shown in Fig. 7) into the chicken breast tissue, with bone elongation in the vertical polarization direction for optical imaging. Line scan images were obtained by linear scanning in the direction perpendicular to the bone elongation, i.e., scanning across the bone. The spatial range in the abscissa is 1.1 cm with the step size of 1 mm. The gray level represents the relative intensity distribution. In Fig. 7, we compare various gating schemes, including (a) time gated integrated intensity (S_0), (b) time-gated S_1 component, i.e., the conventional approach of combining polarization discrimination with time gating, (c) DOP distribution with time gating, and (d) DOP distribution without time gating. As shown in part (d), even a rough image cannot be obtained without time gating. The comparison between parts (a)-(c) shows that although images of the chicken bone were obtained with time gating and/or polarization discrimination, an image of higher resolution and contrast was achieved with DOP evaluation. This result implies that the time-gated DOP measurement can substitute the conventional polarization-discrimination method in filamentous tissues for optical imaging.

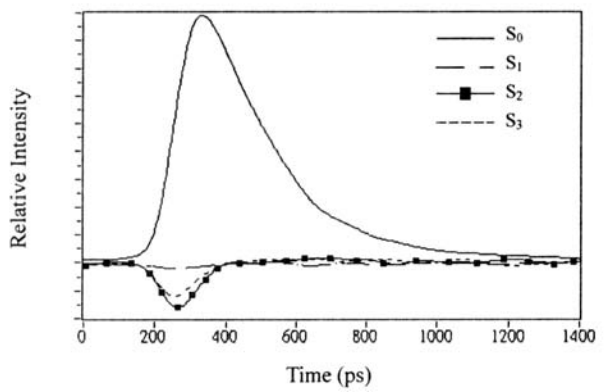

Fig. 6 Time-resolved Stokes element profiles of chicken breast tissue.

5. CONCLUSIONS

In this paper, we first demonstrated the effective-

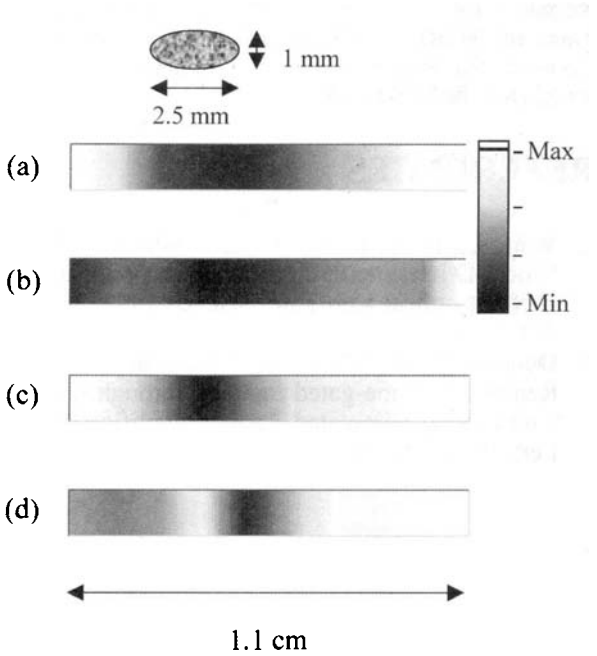

Fig. 7 1-D images of the chicken bone in chicken breast tissue with filament orientation in the horizontal direction: (a) time-gated integrated intensity (S_0), (b) time-gated S_1 component, (c) DOP with time gating, and (d) DOP without time gating.

ness of imaging in a tissue phantom with isotropic scattering by using polarization discrimination combined with time gating. In this situation with pork as target and diluted milk as tissue phantom, the reduced scattering coefficient mapping manifests clear images. However, such an imaging method became less effective in filamentous tissues, such as chicken breast tissues because filamentous tissue had a deterministically anisotropic property. It led to coherent coupling between the two linear polarization components. The coherent coupling resulted in difficulty of using the conventional polarization gating method for optical imaging of filamentous tissues. In this situation, we employed the time-gated DOP imaging technique that based on the Stokes formalism. The results showed that the DOP measurement was quite effective in high-quality imaging of objects in filamentous tissues. The improvement of this method was attributed to the unchanged polarization part under the coupling processes of various polarization components. Because the Stokes vector provides complete polarization information of transmitted light, this technique can be applied to imaging and characterization of other kinds of filamentous tissues.

ACKNOWLEDGEMENT

This research was supported by National Health Research Institute, The Republic of China, under the grant of NHRI-GT-EX89, and by National Science Council, The Republic of China, under grants of NSC 89-2218-E-002-094 and NSC 89-2218-E-002-095.

REFERENCES

1. Wang L., Ho P. P., Liu C., and Alfano R. R.: Ballistic 2-D imaging through scattering walls using an ultrafast optical Kerr gate. Science 1993; 253, 769-771.
2. Duncan M. D., Mahon R., Tankersley L. L., and Reintjes J.: Time-gated imaging through scattering media using stimulated Raman amplification. Opt. Lett. 1991; 16, 1868-1870.
3. Abraham E., Bordenave E., Tsurumachi N., Jonusauskas G., Oberle J., and Rulliere C.: Real-time two-dimensional imaging in scattering media by use of a femtosecond Cr^{4+}:forsterite laser. Opt. Lett. 2000; 25, 929-931.
4. Doule C., Lepine T., Georges P., and Brun A.: Video rate depth-resolved two-dimensional imaging through turbid media by femtosecond parametric amplification. Opt. Lett. 2000; 25, 353-355.
5. Yoo K. M., Das B. B., and Alfano R. R.: Imaging of a translucent object hidden in a highly scattering medium from the early portion of the diffuse component of a transmitted ultrafast laser pulse. Opt. Lett. 1992; 17, 958-960.
6. Wang L., Ho P. P., and Alfano R. R.: Time-resolved Fourier spectrum and imaging in highly scattering media. Appl. Opt. 1993; 32, 5043-5048.
7. Schmitt J. M., Gandjbakhche A. H., and Bonner R. F.: Use of polarized light to discriminate short-path photons in a multiply scattering medium. Appl. Opt. 1992; 31, 6535-6546.
8. Horinaka H., Hashimoto K., Wada K., Cho Y., and Osawa M.: Extraction of qusai-straightforward-propagating photons from diffused light transmitting through a scattering medium by polarization modulation. Opt. Lett. 1995; 20, 1501-1503.
9. Demos S. G. and Alfano R. R.: Temporal gating in highly scattering media by the degree of optical polarization. Opt. Lett. 1996; 21, 161-163.
10. Morgan S. P., Khong M. P., and Somekh M. G.: Effects of polarization state and scatterer concentration on optical imaging through scattering media. Appl. Opt. 1997; 36, 1560-1565.
11. Sankaran V., Walsh J. T., and Maitland D. J.: Polarized light propagation through tissue phantoms containing densely packed scatterers. Opt. Lett. 2000; 25, 239-241.
12. Vander A. J., Sherman J. H., Luciano D. S.: Human Physiology, The Mechanisms of Body Function. Sixth Edition, McGraw-Hill, New York, 1994; 304.
13. Chou C. -P.: Imaging inhomogeneous penetrable media: Electromagnetic inverse scattering and diffuse light imaging techniques. Ph. D. Thesis, National Taiwan University, R.O.C., 2000.